



# Ion beam assisted deposition of an organic light emitting diode electrode

D. Olzon-Dionysio<sup>a,\*</sup>, J.F.D. Chubaci<sup>b</sup>, M. Matsuoka<sup>b</sup>, R.M. Faria<sup>a</sup>, F.E.G. Guimarães<sup>a</sup>

<sup>a</sup> Instituto de Física de São Carlos, Universidade de São Paulo, Caixa Postal 369, São Carlos, 13560-970 São Paulo, Brazil

<sup>b</sup> Instituto de Física, Universidade de São Paulo, Caixa Postal 66318, São Paulo, 05314-970, São Paulo, Brazil

## ARTICLE INFO

Available online 18 January 2010

### Keywords:

IBAD  
OLED  
PLED  
Interface  
Hybrid

## ABSTRACT

This work presents the electro-optical characterization of metal-organic interfaces prepared by the Ion Beam Assisted Deposition (IBAD) method. IBAD applied in this work combines simultaneously metallic film deposition and bombardment with an independently controlled ion beam, allowing different penetration of the ions and the evaporated metallic elements into the polymer. The result is a hybrid, non-abrupt interface, where polymer, metal and ion coexists. We used an organic light emitting diode, which has a typical vertical-architecture, for the interface characterization: Glass/ Indium Tin Oxide (ITO)/Poly[ethylene-dioxythiophene/poly(styrene sulfonic acid)] (PEDOT:PSS) /Emitting Polymer/Metal. The emitting polymer layer comprised of the Poly[(9,9-dioctyl-2,7-divinylene-fluorenylene)-alt-co-{2-methoxy-5-(2-ethylhexyloxy)-1,4-phenylene}] (PFO) and the metal layer of aluminum prepared with different Ar<sup>+</sup> ion energies varying in the range from 0 to 1000 eV. Photoluminescence, Current–Voltage and Electroluminescence measurements were used to study the emission and electron injection properties. Changes of these properties were related with the damage caused by the energetic ions and the metal penetration into the polymer. Computer simulations of hybrid interface damage and metal penetration were confronted with experimental data.

© 2010 Elsevier B.V. All rights reserved.

## 1. Introduction

Organic light-emitting devices (OLEDs) based on thin polymeric multilayered structures have been subject of growing interest [1]. A vertical architecture, metal/polymer/oxide, is usually used. The injection of balanced charge at both ends depends primarily on the difference of layers work function [2]. For most polymers significant difference in the barrier height at the polymer/cathode and polymer/anode interfaces results, usually, in unbalanced hole and electron injections, which may hinder the OLEDs quantum efficiency. The use of hole/electron injection layer between the luminescent polymer and the oxide/metal, gives rise to benefits in the injection of charge carriers, resulting in an enhancement of the device light emitting properties. It is generally accepted that such hole/electron transport layers modifies the carrier injection properties and block the flow of carriers with opposite polarity into the emissive layers [3,4]. At the cathode interface, a Schottky junction can be formed due to the very low work function of conjugated polymers [5]. A better match of work functions would be achieved using low-work-function metal for the cathode, such as Ca and Mg. However, these metals are very reactive [6]. Some studies about the polymer/metal interface suggest that the early monolayers are doped with metals [7,8]. On the other hand Giro *et al.* [9] used classical molecular simulation and obtained that the

polymer doping should not be expected for some metals, so that this strong beneficial effects have probably a different origin. In this context, it is important to understand, in more details, all factors that promote or affect the enhancement of OLEDs luminescence.

Usually the cathode preparation in OLEDs uses the thermal evaporation process. The use of sputtering method is not usual, due to the organic devices extreme sensibility to radiation, heating and charging effect [10], although the use of a buffer layer avoids these kind of issue [11]. Ion beam assisted deposition (IBAD) is a technique that combines ion beam bombardment with simultaneous metal vapor deposition [12]. It have been used to produce a cathode that acts like a encapsulating layer, obtaining a dense layer that can act as a barrier to moisture and oxygen. A buffer layer was also used in this case, to avoid the possible damages caused by the ion bombardment [13,14]. Although the damage caused by the ion kinetic energy transfer seems to be accepted without further questioning, the damage mechanism and the effect on the devices performance is not clear [15].

In this work, OLEDs were produced using the IBAD to obtain an aluminum cathode. No buffer layer was used, resulting in a deliberated hybrid layer in the polymer-metal interface. Monte-Carlo type simulations were performed using TRIM code (Transport of Ions in Matter) [16] and gives preliminary information about the depth of metal penetration into the active layer and modifications near the interface of this layer. The degradation of the active layer and its emissive property were examined with photoluminescence (PL) measurements. Current–Voltage (*I*–*V*) and Electroluminescence (EL)

\* Corresponding author. Tel./Fax: +55 16 3373 9792.

E-mail address: [dolzon@gmail.com](mailto:dolzon@gmail.com) (D. Olzon-Dionysio).

experiments were carried out to characterize the OLEDs electron injection and electroluminescence properties.

## 2. Experimental procedure

ITO (Delta Technologies) coated glass was used as substrate for the OLEDs. The cleaning procedure includes sonication in acetone, treatment in aqua regia solution and rinsing in milli-Q water. After the ITO cleaning procedure, PEDOT:PSS (Bayer AG) and PFO (ADS 108GE, American Dye Source) were deposited by spin coating, having the thickness around 40 nm and 60 nm, respectively. The deposition of the aluminum layer was carried out in the IBAD system, which consists of a chamber with an e-beam evaporator and a Kaufman-type ion source, where argon ions were used because of its inert properties. The aluminum layer was deposited as stripes due the use of a mask. The amount of evaporated aluminum was measured by a quartz crystal thickness monitor, and in all samples this amount corresponds to a 100 nm non assisted film. The ion beam reaches the surface of the substrate with a normal incidence with energies varying from 0 to 1000 eV. Table 1 summarizes the main deposition parameters. The incident angle, relative to the substrate, of the evaporated aluminum was 45°. For higher energies the ion beam current density increases, therefore the deposition rate was also increased to keep constant the ratio between these two parameters. The cathode deposition was held under room temperature and temperature variation during the process is negligible. For sample 1 the ion beam assistance was not used, so this thermal evaporated cathode was used as reference.

PL measurements were recorded by a spectrofluorophotometer RF-5301PC, from SHIMADZU. The excitation wavelength was 490 nm, which corresponds to the maximum absorption wavelength for PFO. The *I*-*V* characteristics were measured with a 370 A Curve Tracer, from Tektronix and a photodiode coupled to a Keithley 617 electrometer were used to measure the electroluminescence produced by Keithley 2400 source.

## 3. Results and discussion

We carried out simulations using TRIM code [16], which is basically based on the effects of pair collisions of implanted ions with substrate. We used a progressive method to reproduce the layer deposition. We started with the atomic composition of the PFO (48 C, 66 H and 2 O) as substrate and the simulation considered 10,000 Ar<sup>+</sup> ions with the desired energy. Afterwards the same simulation was performed for a 10 Å thick aluminum layer deposited on the PFO layer. This configuration allows the ion penetration through the aluminum to the PFO layer. The thickness of aluminum layer was successively incremented until the complete stop of the ions by the aluminum layer, without reaching the PFO substrate. Initially we studied the damage caused by the ions in the PFO. The displacement of the aluminum and PFO carbon atoms caused by the energetic Ar<sup>+</sup> ions were analyzed. Fig. 1 presents the carbon atoms displaced from their original sites in the simulation for the case of an aluminum layer thickness of 20 Å. It is important to note that the ions with 200 eV do not produce any substantial carbon displacement. The same cannot be observed for the other ion beam energies, since the PFO layer is strongly modified along the whole film thickness.

**Table 1**  
Parameters of the deposition.

Sample	Ion beam energy (eV)	Deposition rate (Å/s)	Ion beam current density (μA/cm <sup>2</sup> )	Temperature rise (K)
1	0	1.0	0	0
2	200	1.0	37.6	2
3	600	1.5	56.4	4
4	1000	1.5	56.4	16

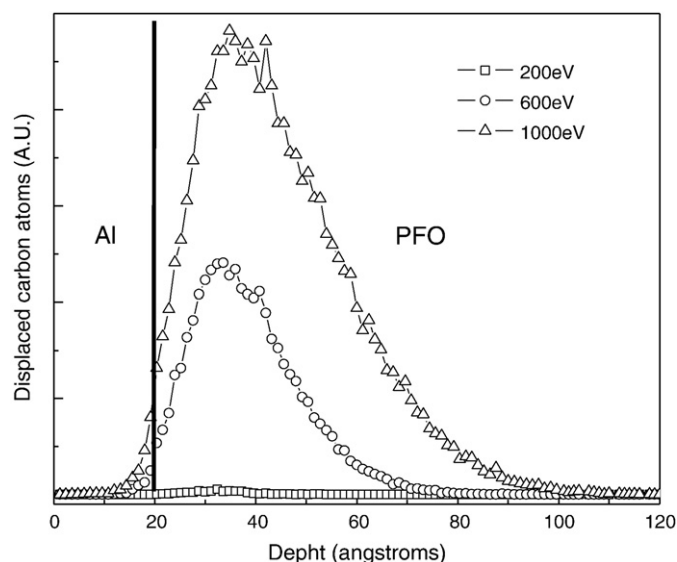


**Fig. 1.** Simulation of the carbon displacement for different ion energies. Ions incidence from the left to the right. Vertical line represents interface between aluminum and PFO.

In the same way, Fig. 2 compares the displacement of the aluminum in both 20 Å thick aluminum top layer (on the left side) and PFO layer (on the right side) for the same Ar<sup>+</sup> ion energies presented in Fig. 1. Besides the strong modification of the aluminum top layer, we observe an appreciate penetration of aluminum atoms in the PFO layer and a non-abrupt interface is formed, where polymer and metal atoms coexists. An upper limit for the penetration can be observed for the aluminum penetration in the PFO layer for Ar<sup>+</sup> ion energies varying between 600 eV and 1000 eV. Ar<sup>+</sup> ions can also sputter some aluminum atoms, this sputtering rate increases as the ion energy rises [17]. As consequence, a further reduction of the aluminum film thickness is expected as energy rises. The displacement of the aluminum in the simulation is related to the mechanism of densification [17] of the aluminum layer. The aluminum layer thickness required to avoid Ar<sup>+</sup> ion penetration in the PFO active layer was also estimated. Aluminum buffer layer thicknesses of 80, 50 and 30 Å prevent the penetration of Ar atoms with energies of 1000, 600 and 200 eV, respectively, in the PFO layer.

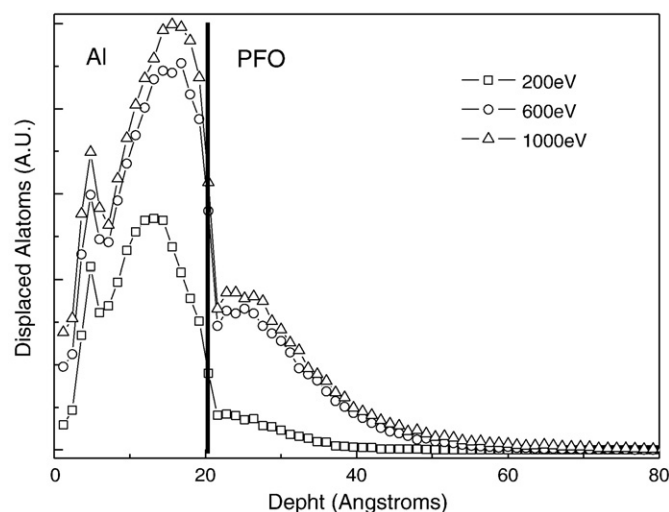


**Fig. 2.** Simulation of the aluminum displacement for different ion energies. Ions incidence from the left to the right. Vertical line represents interface between aluminum and PFO.

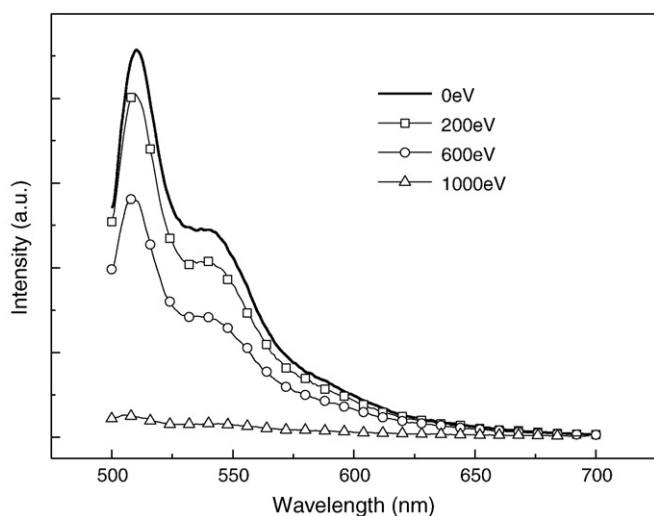


Fig. 3. PL measurement (excited with 490 nm).

Fig. 3 compares the photoluminescence spectra of the PFO measured from the glass/ITO side and below the aluminum electrode for  $\text{Ar}^+$  ion energies of 0 (reference), 200, 600 and 1000 eV. As expected from the simulation, strong dependence of the PFO emission with the  $\text{Ar}^+$  ion beam energy is observed. Besides the intensity decrease and spectral shift of the zero-phonon transition around 510 nm for higher  $\text{Ar}^+$  ion energies, no changes in the vibronic progressions of the PFO was detected. It suggests that modifications of the PFO chain are taking place during the IBAD process for  $\text{Ar}^+$  ion energies higher than 600 eV. In addition, the blue shift of the emission indicates a decrease of PFO conjugation length, which can be accounted for the braking of conjugation due to disorder or chain disruption. The 200 eV sample lost nearly 11% of PL intensity compared to the 0 eV (cathode deposition without  $\text{Ar}^+$  ion assistance). Further decrease of the luminescence intensity is mainly explained by the detuning of the absorption maxima (not shown) due

to the decrease of the mean conjugation length than by the introduction of non-radiatively active defects during IBAD.

The variation of the interface properties with IBAD process can be better followed through the  $I$ - $V$  and EL characteristics presented in Fig. 4(A) and (B), respectively. In Fig. 4 (A), a voltage threshold of about 8 V is obtained for the reference OLED (0 eV) and a modest improvement of the  $I$ - $V$  characteristics can be obtained for the OLED prepared with 200 eV  $\text{Ar}^+$  ion beam assistance. This indicates that the formation of a non-abrupt Al/PFO interface favored the electron injection. Further increase of the  $\text{Ar}^+$  ion beam energy degraded the device characteristics and a short circuit is formed for the OLED prepared with 1000 eV beam, possibly caused by the strong penetration of aluminum atoms in the PFO layer due to the decreasing of the cathode thickness caused by sputtering. In Fig. 4 (B) the EL characteristics of the 600 eV sample shows a weaker electroluminescence and also a later turn-on, compared to the 0 eV sample, as expected. Compared to the 0 eV sample, the 200 eV sample has initially a very similar behavior until around 9 V from there it presents a greater luminance.

#### 4. Conclusions

Damage caused to PFO polymer presents in OLED was examined during the IBAD type deposition of aluminum electrodes. The luminescence measurements show that for higher  $\text{Ar}^+$  ion energies (600 eV and 1000 eV) the damage on the polymer affects significantly the order and braking of PFO conjugation length, which affects the light emissive properties of the polymer. Low energy (200 eV)  $\text{Ar}^+$  ions cause small changes in the emission properties of PFO. TRIM simulations supported these results. Concerning the electron injection properties of aluminum electrode in OLED devices, a modest improvement of the  $I$ - $V$  characteristics for IBAD process with 200 eV  $\text{Ar}^+$  ion beam indicates that the formation of a non-abrupt interface favors electron injection, which plays a important rule for higher currents, as shown by the higher electroluminescence achieved by the 200 eV sample For IBAD performed with 1000 eV ions, the cathode became unusable, probably due to the sputtering effect caused by the incident ions.

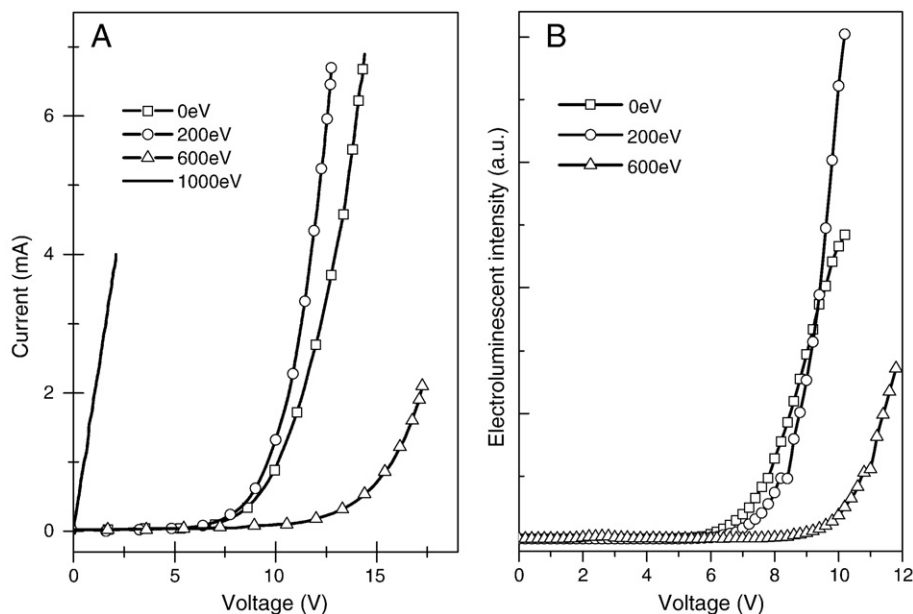


Fig. 4. A)  $I$ - $V$  characteristics and B) EL characteristics.

## Acknowledgements

The authors are grateful to the financial support from CNPq, (Proc. 135349/2009-5) INEO (MCT) and FAPESP. They also acknowledge the support given by Gerson dos Santos, Gregório Couto Faria and Gonçalo Pedro Golçalves with the electroluminescence measurements.

## References

- [1] R.H. Friend, et al., *Nature* 397 (1999) 121.
- [2] L.S. Hung, C.H. Chen, *Mater. Sci. Eng., R* 39 (2002) 143.
- [3] X. Gong, D. Moses, A.J. Heeger, *Appl. Phys. Lett.* 83 (2003) 183.
- [4] X. Jiang, Y. Liu, D. Zhu, *Solid State Comm.* 99 (1996) 183.
- [5] M. Meier, S. Karg, W. Riess, *J. Appl. Phys.* 82 (1997) 1961.
- [6] T.M. Brown, F. Cacialli, *J. Polym. Sci., Part B: Polym. Phys.* 41 (2003) 2649.
- [7] J.M. Bharathan, Y. Yang, *J. Appl. Phys.* 84 (1998) 3207.
- [8] M.B. Huang, K. McDonald, J.C. Keay, Y.Q. Wang, S.J. Rosenthal, R.A. Weller, L.C. Feldman, *Appl. Phys. Lett.* 73 (1998) 2914.
- [9] R. Giro, M.J. Caldas, *Phys. Rev. B* 78 (2008).
- [10] L.S. Hung, L.S. Liao, C.S. Lee, S.T. Lee, *J. Appl. Phys.* 86 (1999) 4607.
- [11] S. Kho, S.J. Bae, D.G. Jung, *J. Mater. Res.* 17 (2002) 1248.
- [12] Y. Andoh, Y. Suzuki, K. Matsuda, M. Satou, F. Fujimoto, *Nucl. Instrum. Methods Phys. Res. B* 6 (1985) 111.
- [13] M. Chakaroun, R. Antony, P. Taillepiere, A. Moliton, *Mater. Sci. Eng., C* 27 (2007) 1043.
- [14] S.M. Jeong, W.H. Koo, S.H. Choi, H.K. Balk, *Solid State Electron.* 49 (2005) 838.
- [15] L.S. Liao, L.S. Hung, W.C. Chan, X.M. Ding, T.K. Sham, I. Bello, C.S. Lee, S.T. Lee, *Appl. Phys. Lett.* 75 (1999) 1619.
- [16] J.P. Biersack, L.G. Haggmark, *Nucl. Instrum. Methods* 174 (1980) 257.
- [17] D.M. Mattox, *J. Vasc. Sci. Technol. A* 7–3 (1989) 1105.